Tang, Xianqiang; Li, Rui; Wu, Min; Zhao, Weihua; Zhao, Liangyuan; Zhou, Yinjun; Bowes, Michael J. 2019. **Influence of turbid flood water release on sediment deposition and phosphorus distribution in the bed sediment of the Three Gorges Reservoir, China.**

Influence of turbid flood water release on sediment deposition and phosphorus distribution in the bed sediment of the Three Gorges Reservoir, China

Xianqiang Tang[a,b*], Rui Li[a,b], Min Wu[a,b], Weihua Zhao[a,b], Liangyuan Zhao[a,b], Yinjun Zhou[b], Michael J Bowes[c]

[a] *Basin Water Environmental Research Department, Changjiang River Scientific Research Institute, Wuhan 430010, China*

[b] *Key Lab of Basin Water Resource and Eco-Environmental Science in Hubei Province, Wuhan 430010, China*

[c] *Centre for Ecology & Hydrology, Wallingford OX10 8BB, UK*

**Corresponding author. Email: ckyshj@126.com* (XianqiangTang).

ABSTRACT

Excessive phosphorus (P) loading was identified as an urgent problem during the post-Three Gorges Reservoir (TGR) period. Turbid water with high suspended sediment loads has been periodically released during the flood season to mitigate sediment deposition in the TGR, but limited attention has been paid to its effect on the distribution of P in bed sediment within the reservoir. In this study, field surveys, historical monitoring data related to sediment deposition, and physiochemical properties and the fractional P content in the mainstream surface sediment and representative column sediment, were used to investigate the effect of turbid flood water release on P distribution in bed sediment. The results revealed that turbid flood water release could discharge approximately 20 % of the suspended sediment inflow entering the TGR. Additionally, both the particle size of the inflow sediment and suspended sediment flux tended to decline, and the deposited sediment volume tended to constantly increase in the TGR at a rate of 0.117 billion tonnes per year between 2004 and 2016. The median particle size (MPS) was larger for surface sediment obtained in the flood season than for that obtained in the dry season, and the MPS tended to increase with an increase in the sediment depth from 0 to 20 cm. The total phosphorus (TP) content in sediment ranged from 2.6 % to 17.5 % lower in the flood water releasing period than in the non-flood water storing period. However, no consistent variation was detected for the vertical distribution of P fraction in the top 20 cm of bed sediment. Compared with lakes with slow deposition rates, the TGR showed a rapid sedimentation rate of more than 1.0 m/y, which mostly resulted in the uniform distribution of the surface sediment P fraction.

Keywords: Three Gorges Reservoir; deposition; distribution; fractional P; fine particles; reservoir management

1. Introduction

P has been identified to being primarily responsible for the eutrophication of the Three Gorges Reservoir (TGR) (Fu et al., 2010; Han et al., 2018). Excessive P within the mainstream sections of the TGR is one of the most urgent environmental problems since its construction (Zhuo et al., 2017a). Sediment is not only an important carrier for particulate phosphorus (PP) but also a key environmental component for the aquatic ecosystem. The construction of the Three Gorges Dam (TGD) changed the natural hydrological regime of nearly 600 km upstream river channel (Cao et al., 2011), and caused the selectivity and discontinuity of transportation for different size of sediment particles. A study indicates that after the dam became fully operational, more than 75 % of PP and suspended sediment (SS) could be trapped in the TGR even during the flood season (Tang et al., 2018a). Retention and regulation of sediment by the TGD unavoidably affect the P distribution dynamics and bioavailability for sediment of the TGR.

Economic growth and rapid urbanization in this region have generally led to increased P discharge and have resulted in increasing P loads in the surface sediment of the reservoir. For most eutrophic lakes, weak hydrodynamic conditions including slow water flow and long water retention time favor the enrichment of P within sediments, which exhibit a vertical enrichment pattern (Ribeiro et al., 2008; Liu et al., 2015). For TP, the upper 0-10 cm sediment layer typically contains much higher levels of 1463.47 mg/kg than 853.83 mg/kg in the lower 10-20 cm sediment layers, and the most heavily contaminated sediment layer is the top 0–5 cm, where P is mobile and easily released to the overlying water column (Wu et al., 2011). In contrast to lakes, in the TGR, low turbidity water is stored in the dry season and water with high suspended sediment load is discharged in the wet season to both prevent sediment deposition (Li et al., 2015a) and ensure continued sediment supply to the river downstream. The hydrodynamic process in the flood season may flush the reservoir bed and transport a part of the bed sediment (BS) and SS downstream through the TGD. Therefore, high-turbidity flood water discharge in the wet season is thought to regulate the distribution of P in sediment in the TGR; however, the effects of the discharge are still unclear.

Previous studies have focused on P distribution in surface sediment or in soil obtained from tributaries and water fluctuating zones (Wang et al., 2009; Luo et al., 2015; Zhuo et al., 2017a; Pan et al., 2018). Accumulation of PP in the parts of surface sediment in these environments increases the potential ecological risk in the reservoir due to sediment P release (Wang et al., 2009; Wang et al., 2015; Han et al., 2018). The sediment or soil in the water level fluctuating zone of the TGR exhibits a seasonal change between the "sink" and "source" for P, and soil organic phosphorus (Org-P) and Fe/Al oxides bound phosphorus (Fe/Al-P) are the major contributors to the released P (Zhang et al., 2012a). Other researchers have investigated and evaluated sediment or soil P distribution status in tributaries, such as the Daning River, Xiangxi River, and Pengxi River (Wang et al., 2009; Luo et al., 2015; Huang et al., 2017). Moreover, P does not notably accumulate in the reservoir's mainstream surface sediment when impoundment water level increases from 135 to 175 m (Tang et al., 2018b). However, limited information on the P distribution status for deposited column sediment in the mainstream TGR is available.

The impoundment of the TGR promotes sediment deposition; the annual sediment deposition volume increased from 12.40 million tonnes in 2003 to 19.60 million tonnes in 2010 (Changjiang Water Resource Commission [CWRC], 2000–2016). The implementation of water and soil conservation measures, and the trapping of sediment by upstream reservoirs have reduced the particle size and load of sediment entering the TGR (Cao et al., 2011). The median particle size (MPS) of SS in the mainstream sections of the TGR decreased from 0.011 to 0.009 mm between 2003 and 2010 compared with the values acquired in the 1990s (CWRC, 2000-2016).

In the TGR, fine silt contains higher P content than coarse sand because fine particles tend to adsorb more P due to their higher surface area: volume ratio (Han et al., 2018). Moreover, relatively high sediment organic matter (OM) and Fe/Al hydroxides in fine particles resulted in a high P concentration in bed sediment (Tang et al., 2014). An increase in the proportion of fine particles may encourage the enrichment of P in bed sediment; however, no obvious increase in the TP content in surface sediment is observed during the post-TGR period compared with that in the pre-TGR period (Zhuo et al., 2017a; Pan et al., 2018). Therefore, whether the releasing turbid flood water and storing clean water causes the irregular distribution of P in sediment of the TGR is unclear.

Sediment components are closely related to P storage dynamics (Tang et al., 2014). The profile distribution of the key sediment physiochemical properties can reflect historical changes in the sedimentation process. Moreover, the vertical distribution of sediment P fractions may reveal the effects of the impoundment and operation of the TGD on the sedimentation and deposition of P.

Sediment deposition mainly drives and determines the P storage and distribution, and presence of TGD caused a great amount of sediment deposition and associated P retention. In lakes and reservoirs, deposited sediment usually plays a major role in the P cycle and acts as a sink, or a source that carries out chemical reactions and transfers through the interface between water and the sediment layer (Jarvie et al., 2005). Sediment particles deposition and retention significantly impacted on the P transportation and enrichment, and sediment physic-chemical properties effectively regulate the P bioavailability. More than 90 % of the SS with MPS smaller than 0.01 mm deposited in the permanent backwater zones of the TGR, and these trapped fine sediment particles with relative high P contents are hard to flush due to their excellent adhesiveness (Li et al., 2016). Sediment P retention, distribution and bio-available fractions release play an important role in the maintenance of trophic regime in the TGR (Wu et al., 2016), and sediment P release can be mostly influenced by water depth, P species, water temperature, pH, oxidation-reduction potential, organisms, bacteria and hydrodynamics (Chen et al., 2016; Wu et al., 2017).

In this study, the status of sediment retention and deposition in the mainstream sections of the TGR during the post-TGR period were evaluated, and the differences in surface sediment physiochemical properties and P fractions during flooding and dry seasons were identified. Moreover, the depth profile of sediment physiochemical parameters and P fractions in deposited column sediment samples from representative mainstream sections of the reservoir was determined. This study assessed the effects of high-turbidity flood water discharge on sediment retention and P distribution in the TGR and provided valuable information for management of P stored in sediment during the post-TGR period.

2. Materials and methods

2.1 Sample collection and preparation

The TGR extends across the reach of the Changjiang River between Jiangjin of

Chongqing City and Yichang of Hubei Province (Fig 1), covering a distance of 570-650 km. A staged impoundment scheme was adopted for the TGR to mitigate the potential negative effects of this reservoir's operation on the ecological environment. The maximal impoundment water level was 135, 156, and 175 m in 2003, 2006, and 2010, respectively (Wang et al., 2013). The TGR has been fully operational since 2010, with the water level fluctuating between 145 m in the wet season (from April to September, for releasing turbid flood water) and 175 m in the dry season (from October to mid-April in the following year, for storing clear water).

Surface sediment collection: Approximately 1.0 kg of surface sediment samples (top 10 cm) were collected in triplicate using a grab style sampler in October 2016, June 2017, and December 2017, and the corresponding impoundment water levels were 175, 145, and 175 m. During the dry season, 10 surface sediment samples from the reservoir were obtained at Chongqing (CQ), Changshou (CS), Fuling (FL), Zhongxian (ZX), Yunyang (YY), Fengjie (FJ), Badong (BD), Xiangxi (XX), Zigui (ZG), and Maoping (MP); these sections were 619.1, 538.1, 489.2, 370.2, 252.2, 169.3, 76.4, 31.0, 24.3, and 2.5 km upstream from the TGD, respectively. All sampling sites (Fig. 1) were located at representative sections selected according to the Code for Reservoir Hydrologic and Sediment Surveys (SL 339-2006) (MWR, 2006). Due to fast flow in the upstream sites during the flood season (sediment samples will be dispersed and lost during sampling due to fast flow), surface sediment samples were only obtained from YY, FJ, BD, XX, ZG, and MP in June 2017.

Column sediment collection and preparation: In October 2016, at YY, FJ, BD, XX, and ZG, samples of column sediments to a depth of 20 cm were obtained using a self-made gravity corer equipped with two parallel acrylic liners with an inside diameter of 10 cm. Column sediments were immediately cut into 2-cm sub-samples at the point of collection, and then each sub-sample was fully blended.

All sediment samples were transported to the laboratory on the same day as collection within sealed plastic bags and stored in a portable refrigerator at 4 °C (Zhang et al., 2012b). Each sample was divided into two parts: one was used to determine the particle size distribution, and the other was air-dried and sieved using 100-mm-diameter meshes to analyze sediment pH, organic matter (OM), mineral compositions, and the concentration of P fractions.

2.2 Sediment physicochemical property and P fractions determination

OM was determined by loss on ignition, and more details are given in Tang et al. (2014). Sediment particle size distribution was determined using a HORIBA-950V2 laser diffraction particle size analyzer. Mineral compositions of the sediment samples were determined through powder X-ray diffraction (XRD) analysis by using a D8 advance diffractometer (Bruker AXS, Inc). XRD patterns were recorded using Ni-filtered Cu K_{α} radiation (step size, 0.02 °/s; operating voltage, 40 kV; scan range, 2θ=5–65 °).

The sequential extraction of P was performed to quantify the concentration of the

P species. Twenty-five milliliters of 1 mol/L NH_4Cl was added to 500 mg of sediment (dry weight equivalent), and the suspension was shaken for 0.5 h. After shaking, the suspension was centrifuged at 3000 rpm for 10 min, and the supernatant was decanted. This process was repeated with 0.5 mol/L NH_4F (shaken for 1 h), 0.1 mol/L NaOH (shaken for 2 h and then shaken again for 2 h after standing for 16 h), 0.3 mol/L $Na_3C_6H_5O_7 \cdot 2H_2O$ (shaken for 0.5 h), and 0.5 mol/L H_2SO_4 (shaken for 1 h); these fractions represented exchangeable phosphorus (Ex-P), phosphorus bound by Al oxides (Al-P), phosphorus bound by Fe oxides (Fe/P), occluded phosphorus (O-P), and calcium-bound phosphorus (Ca-P), respectively. The TP content within the sediments was determined with the Standards, Measurements and Testing (SMT) protocol, by heating the sub-sample at 720 °C, followed by 3 mol/L H_2SO_4 extraction (Ruban et al., 2001). All P fractions were measured using the ammonium molybdate spectrophotometric method (APHA, 1998).

2.4 Historical data collection and analysis

Measurements of all sediment samples were conducted in triplicate. All instruments conformed to national measurement standards, and reference materials and standard reagents were used for quality control.

Historical monitoring data of flow rate, water level and sediment delivery ratio in the TGR during the flood season between 2003 and 2010 were collected from the Bureau of Hydrology, Changjiang Water Resources Commission. Sediment deposition data on typical sections for the TGR a the distance of 5.6 km, 160.1 km, and 431.3 km to the TGD in October 2003, 2011, and 2012 were also obtained from the Bureau of Hydrology, Changjiang Water Resources Commission. Moreover, sediment delivery ratio, accumulated deposition volume, and annual sediment flux for the TGR between 2004 and 2016 were collected from the Changjiang Sediment Bulletin (CWRC, 2000–2016). Annual average flux, concentrations and MPS of SS at national controlled hydrological sections of Cuntan and Yichang during the pre-and post-TGR period were also obtained from the Changjiang Sediment Bulletin (CWRC, 2000–2016). Relationships between bioavailable phosphorus (Bio-P) in column sediment and the MPS and OM were analyzed using Origin 8.0 software.

3. Results and discussion

3.1 Sediment deposition characteristics

Impoundment of the TGR considerably changed the hydrodynamic conditions for SS transportation in the ~600 km natural river reach, where formed the reservoir after the presence of the TGD. Average flow velocity during the post-TGR period (2003-2010) was between 0.09 and 2.43 m/s, which was substantially lower than that of 3–5 m/s observed in natural river channels (CWRC, 2000–2016). The reduction of water velocity facilitated the sedimentation and deposition of SS within the reservoir. Releasing high-turbidity water during the flood season is thought to reduce, rather than avoid, SS deposition; the measured sediment volume in the TGR continually increased from 0.102 billion tonnes in 2004 to 1.523 billion tonnes in 2016, with an annual augmentation of 0.117 billion tonnes (Fig. 2).

Sediment depositions in the TGR are mostly related to three factors: operational water level in the flood season, upstream runoff, and SS loads. Lower flow velocity usually means lower SS carrying capacity, and during the flood season, a lower operational water level causes higher water flow, which favored SS discharge. During the staged impoundment period (2003–2010), the lowest daily average flow and operational water level resulted in the lowest SS deposition volume of 0.112 billion tonnes (Table 1, recorded in 2006). However, the highest daily average flow and operational water level caused the maximal SS deposition volume of 0.229 billion tonnes (recorded in 2010; Table 1, Fig.2). Furthermore, effective SS trapping by upstream large cascade reservoirs and implementing appropriate water and soil conservation measures caused a marked decline in the size and loads of SS entering into the TGR (Mao et al., 2012; Cao et al., 2011). This led to a continually decreasing trend in the sediment deposition volume from 0.229 billion tonnes in 2010 to 0.042 billion tonnes in 2016 (Fig. 2).

Most (98.4 %) of the total sediment in the TGR has been transported in the form of SS; moreover, 90 % of the total SS transportation and retention in the TGR occur during the flood season (Mao et al., 2012). The sediment delivery ratio can be used to evaluate effect of turbid flood water release on mitigating SS deposition. The operational water level during the flood season is closely related to the sediment delivery ratio. The sediment delivery ratio continually decreased from almost 40 % in

2004 to less than 15 % in 2010 (Fig. 2), with the mean water level correspondingly increased from 135.10 to 153.60 m (CWRC, 2000–2016). Sediment delivery ratios showed an increasing trend after the TGR became fully operational (2010; Fig. 2). One possible explanation is that the successive impoundment of the upstream large dams of Xiangjiaba and Xiluodu in 2012 and 2013, respectively, resulted in a further decline in inflowing SS loads.

Annual sediment volume deposited in the TGR continuously decreased from 0.219 billion tonnes in 2012 to 0.042 billion tonnes in 2016. Trapping of sediments by an upstream cascade may increase the proportion of fine sediment particles contained in the inflow and may thus improve the SS discharge capacity. This phenomenon probably caused the sediment delivery ratio to increase to 20 % in 2012, which was higher than the ratio of 14.3 % obtained in 2010 (Fig. 2).

The presence of the TGD and the release of high-turbidity flood water in the wet season changed sediment transportation process along the mainstream sections of the Changjiang River. The nationally controlled hydrologic section of Cuntan was selected to investigate variations in sediment inflow. Annual average SS flux, concentrations, and MPS decreased from 0.43 billion tonnes, 1.24 kg/m^3, and 0.011 μm during the pre-TGR period to 0.20 billion tonnes, 0.60 kg/m^3, and 0.009 μm during the post-TGR period, representing corresponding reductions of 53.5 %, 51.6 %, and 18.2 % (Table 2). The Yichang section was used to evaluate the SS retention capacity of the TGD. The reductions of annual average sediment flux, concentrations, and MPSs were 89.8 %, 87.6 %, and 55.6 % from the pre- to post-TGR period (Table 2).

The TGR exhibited a powerful SS retention capacity even though both upstream inflow SS loads and particle sizes tended to decline. TGD mostly trapped SS with a MPS more than 0.01 mm (Li et al., 2015b), and flocculation and sedimentation of fine sediment particles mainly caused the decline in the MPS of the SS discharged downstream, which may have resulted in the MPS decreased from 0.009 μm during the pre-TGR period to 0.004 μm during the post-TGR period for the Yichang Section (Table 2).

3.2 Variation in sediment physiochemical properties

Sediment physiochemical properties are closely related to the periodic release of turbid flood water. To investigate the difference in sediment disposition under the maximal and minimum impoundment water levels of 175 and 145 m, respectively, 0–10 cm of surface sediment obtained for an entire hydrologic year was analyzed. The sediment MPS gradually decreased from approximately 24 μm at the upstream site at CQ to less than 9 μm at MP (2.5 km upstream of the TGD) (Fig. 3). Overlapping curves of sediment MPS distribution for October 2016 and December 2017 indicated no significant difference in annual sediment deposition at these aforementioned sections. Impoundment water levels greatly affected particle sedimentation, and surface sediment MPS was generally larger under a lower impoundment water level of 145 m in June 2017 compared with 175 m in October 2016 and December 2017

(Fig. 3). This indicates that more fine particles were transported during the non-flood season than that during the flood season. Fine particles generally contain much more OM than large particles (Tang et al., 2014). OM distribution in fine particles was opposite to the MPS distribution, and surface sediment obtained in the lower river reach had considerably more OM than upper river reach sediment. This OM distribution pattern also indicated that slow flow velocity resulting in nutrient accumulation when a dam is present (Wu et al., 2011; Miller, 2012).

The column sediment samples showed weak alkaline pH values, ranging from 7.39 to 7.59 (Table 3), which demonstrated the enrichment of calcareous minerals (Pan et al., 2016). No marked difference was noted in mineral components among the five column sediment sampling sites (Table 3). Chlorite, illite, and quartz were the main sediment components, and their average proportions to the total sediment mass were 26.0 %–31.0 %, 19.9 %–28.0 %, and 21.3 %–24.0 %, respectively. Sediment with a smaller MPS had higher OM and chlorite content (Table 3). This may be because fine particles contain more clay, silt, and weatherable minerals (Li et al., 2012a). A representative column sediment sample taken from YY (in the central section of the reservoir, 252.2 km upstream of the TGD) was selected to determine the vertical distribution of OM, MPS, and sediment components, it is indicated that silt (4–63 μm) and fine sand (>64 μm) dominated sediment fractions, and fine sand accounted for more than 60 % of the total sediment mass (Fig. 4). Moreover, the MPS tended to increase slightly with an increase in the sediment depth; this suggests that sediment particles deposited during the middle stage of the wet season were much larger than those trapped during the final stage of the wet season.

Approximately 99 % of SS deposited in the TGR was stored in the permanent backwater area, 524 km river reach upstream of the TGD (Li et al., 2015b). Hu et al. (2013) reported that the MPS of trapped sediment was generally less than 0.01 mm; this result is comparable with that of our study. Sedimentation of coarse particles due to a decline in flow velocity caused surface sediment along the mainstream sections of the TGR to become small and fine. As a result, sediment with a smaller MPS was detected in the lower river reaches (Fig. 3). Li et al. (2015b) found that SS deposition in the TGR was discontinuous, and that majority of the SS was deposited in the wide valley and curved river channels. Therefore, releasing turbid flood water may have different effects on sediment deposition along the mainstream of the TGR. Moreover, multiple sources (upstream and 33 tributaries of the TGR) of SS inputs and complex conditions of river BS erosion and siltation further complicated the irregular distribution of the major physiochemical properties of column sediment.

3.3 Phosphorus distribution dynamics for sediment

Turbid flood water release considerably affects P distribution in surface sediment. Regardless of the wet or dry season, TP, Fe/Al-P, and Ca-P were constantly higher at the uppermost site at CQ than at the other sampling sites (Fig. 5). Sampling site CQ drains a watershed where urban domestic wastewater and agricultural runoff for Chongqing City are major sources of P. Except for CQ, no obvious trend for the distribution of TP, Fe/Al-P, and Ca-P along the mainstream sections of the TGR was observed. Differences in P distribution under different impoundment water levels were noted, and the TP content in sediment was 2.6 %–17.5 % higher in the turbid flood water releasing period (June 2016) than in the clean water storing period (October 2016 and December 2017; Fig. 5). Inflow to the TGR usually carries more PP associated SS during the wet season than during the dry season (Tang et al., 2018a), surface sediment TP loads were theoretically higher in the flood season than that in the non-flood season. Zhuo et al (2017a) found that TGR mainstream sediment TP contents fluctuated during different flow periods, however, no regular difference in average sediment TP contents ratio were detected between July and January (Fig. 5). Higher PP loads and coarser particle size in the flood season may result in a comparable sediment TP content with that obtained in non-flood season, when there has relatively low PP loads and fine particle size.

Ca-P has been reported to be relatively stable (Wu et al., 2016), especially in neutral and alkaline environments such as the TGR (Table 3). Fe/Al-P can be exchanged with OH^- and other inorganic P compounds and can be used for the evaluation of algal-available P (Zhou et al., 2001). Sediment Ca-P and Fe/Al-P levels were 3.7 %–25.8 % higher and 3.9 %–25.9 % lower, respectively, during the turbid flood water releasing season than during the clean water storage season.

Mean fractional P content in bed sediment cores revealed the irregular distribution of Ex-P, Fe-P, Ca-P, and TP along the mainstream sections of the TGR (Table 4). The Al-P and O-P content increased from upstream to downstream. No significant difference was observed in the TP content between column sediment and surface sediment (Table 4 and Fig. 5). Bio-P in sediment was calculated by adding Ex-P, Fe-P, and Al-P. Mean Bio-P increased slightly from 38.00 mg/kg at YY to 55.06 mg/kg at ZG. The calculated ratio of Bio-P to TP ranged from 3.9 % to 6.1 %, which was substantially lower than 11.5 %–50.2 % observed for the eutrophic lakes such as Taihu (Jin et al., 2006). A representative column sediment sample taken at YY demonstrated that there was no consistent variation detected for each P fraction when sediment depth increased from 0 to 20 cm (Fig. 6). This was contradictory to the widely reported decline trend of P storage in surface lake sediment (Ribeiro et al., 2008). This phenomenon can be explained: (1) deeper than 20 cm sediment is deposited in one hydrologic year, which will be demonstrated in the following sections, such that there was insufficient time for geochemical processes to develop a P profile; (2) negligible variation occurs in sediment physiochemical properties and water column P loads between different hydrologic years (Lou et al., 2011).

Bio-P can be used to evaluate the potential risk of sediment P release for water column eutrophication (Wang et al., 2015). Regression analysis was conducted to determine the relationship between the Bio-P content in column sediment and key sediment physiochemical parameters such as OM and the MPS. As shown in Fig. 7, Bio-P was positively and linearly related to the OM content (r^2=0.52) but was negatively and exponentially related to the MPS (r^2=0.30). The positive correlation of OM with P adsorption is widely acknowledged (Wang et al., 2007). Moreover, fine particles generally tend to adsorb more dissolved phosphorus (DP) than coarse particles because of the larger surface area in a unit mass (Yao et al., 2016). Fine sand dominated sediment composition (Fig. 4); thus, physical adsorption by fine sediment particles substantially contributed to the P content in sediment (Tang et al., 2014). Therefore, fine sand dominated sediment compositions caused the low Bio-P content was weakly and negatively related to the sediment MPS range of 3.94–12.86 μm.

A variety of factors including sediment chemical and biological properties, benthic bioturation, and aquatic plant activities affects the distribution and bioavailability of P in lake sediments (Chen et al., 2016; Xing et al., 2018; Fan et al., 2018). Unlike shallow lakes, the water depth in the TGR can be achieved 100 m when water level is kept at the normal pool level of 175 m, and redox potential and hydrodynamic conditions greatly controlled the sediment P storage. P in the sediment layer included P bound to the sediment particles and that dissolved in the pore water, and the partitioning is significantly affected by redox conditions (Patrick and Khalid, 1974). P associated with Fe/Al (hydr) oxides is the fundamental Bio-P fraction in the sediment, which is sensitive to the changes in the redox value at the sediment-water interface (Wang et al., 2015). The particulate FeOOH is reduced to the dissolved Fe^{2+} under anaerobic conditions (Huang et al., 2015), and thus resulting in the release of adsorbed phosphorus into the pore water. Moreover, with the increase of water depth, the release of Bio-P from the continuously submerged BS could be accelerated under anoxic conditions. For the TGR, however, previous research indicated that the released Bio-P made a little contribution to concentration of P in the water column (0.1-1.0 ‰), but the long term Bio-P release should be paid more attention if considering the Bio-P removed by the sediment resuspension (Wu et al., 2016) .

3.4 Effect of turbid flood water release on P distribution in sediment

Sediment was the carrier and regulator for water column P. After the release of turbid flood water during the flood season occurred regularly in the TGR, P distribution in sediment was mainly related to inflow sediment loads, sediment delivery ratio, and water column P loads. Sediment volume directly affected P storage capacity. The measured SS deposition in the TGR continually increased with an annual augmentation of 0.117 billion tones between 2004 and 2016 (Fig. 2), though sediment inflow loads tended decline due to effective sediment retention by the upstream cascade reservoir and the large-scale implementation of water and soil conservation practices (Cao et al., 2011). Releasing turbid flood water only contributed to nearly 20 % of the sediment delivery ratio (Fig. 2), and the limited discharge of SS to downstream causing an annual retention of 80 % of the SS inflow, which facilitated the deposition of PP associated SS in the TGR. In addition to the contribution of SS deposition, decreased inflow sediment particle size facilitated P enrichment. An increase in fine particles promoted sediment adsorption and led to an increase in the P content; the P concentration contained in SS was reported to be approximately 20 % higher than that contained in BS (Tang et al., 2018a). This suggests that both the amount and concentrations of the P in surface sediment increased, even though turbid flood water was discharged.

Sediment deposition conditions are closely related to P distribution. Sediment deposition in the TGR shows discontinuous and spot distribution features, with the majority of the siltation occurring in the wide valley, the confluences with tributaries, and on bends in river channels. It is indicated that more than 70 % of the SS deposition occurred in less than one-sixth of the total length of the mainstream channel (Hu et al., 2013). Differences were observed in SS deposition in the TGR due to the variation in the river channel topography (Fig. 8); since the first impoundment in 2003, sediment with a depth of almost 50 m was deposited in some local sections until 2012. Moreover, although the sedimentation curve overlapped between 2011 and 2012, more than 1-m sediment accumulated during a complete hydrologic year (Fig. 8b). Compared with the sedimentation rate of 0.2–0.4 cm/a for most lakes downstream of the TGR (Yao et al., 2006), newly formed thick sediment layers (>1.0 m/a) mainly caused the consistent distribution of fractional P in the 20-cm column sediment (Fig. 6).

After the TGR became fully operational, flow velocity tended to exhibit a uniform spatial distribution in the permanent backwater area. Flow velocity considerably affected SS deposition. Li et al (2015b) investigated the sediment movement on the river bed by using an underwater camera, and they revealed that sediment was deposited once flow velocity was lower than 0.5 m/s, and deposited sediment was flushed once flow velocity exceeded 1.1 m/s. Flow velocity tended to decrease along the mainstream sections of the TGR; average water flow for the lower reaches of CQ was usually below 1.0 m/s, even in the flood season (Tang et al., 2018a). Therefore, due to insufficient energy of water flow, there will be negligible disturbance of the BS and subsequent P release through turbid flood water discharge.

Since the first impoundment in 2003, the TGR exhibited a continuous increase in sediment and phosphorus retention (Fig. 2). In the TGR, most P in mainstream waters are adsorbed by sediment particles and transported in the particulate phase (Withers and Jarvie, 2008). Sediment deposition facilitates the accumulation and enrichment of adsorbed phosphorus at the bed surface and can later be released to the water column due to changes in hydrodynamic conditions. Flocculation accelerates the fine SS particles deposition, and increases the P adsorption capacity to the SS. When SS concentration is larger than 0.3 kg/m^3, some particles flocculates and the extent of flocculation gets larger when sediment concentration increases. Moreover, the maximum diameter of the primary particles which may be affected by flocculation is about 0.022 mm, which means that majority of the fine SS particles may be influenced by flocculation (Wang et al., 2016). Previous study indicated that much higher P retention velocity can be obtained with higher SS concentration (Tang et al., 2018a), and coarse sediment particles preferentially deposited in the fluctuating backwater zones, while fine particles mostly accumulated in the permanent backwater zones (Mao et al., 2012). Hydrodynamics can influence the spatial distribution of sediments, and further affect the spatial patterns of sediment nutrients in the top 10 cm active sediments, where often act as a ‘sink’ for external nutrient loading (Shen et al., 2011). Operational controls such as releasing turbid flood water could minimize nearly 20 % of the SS deposition and P retention. Therefore, most of the P will be accumulated in the region towards the TGD due to slow water flow, and act as a long term source of Bio-P release under the anaerobic conditions. It is necessary to manage the TGR to increase the sediment delivery ratio, and thus reduce the sediment deposition and P retention.

Dissolved water column P is adsorbed and flocculated into SS and then deposited as sediment P loads. The dry density of newly formed surface sediment was approximately 0.9 g/cm^3; thus, the sediment exhibited the features of flocs (Li et al., 2015b), which suggests the occurrence of flocculation and sedimentation in fine sands. Annual average water column TP concentrations during the flood seasons between 2004 and 2010 were 4.7 % lower than those observed between 1997 and 2003, and retention of PP resulted in an augmentation of DP proportions (Lou et al., 2011). Moreover, increasing fertilizer use enhanced nonpoint source pollution (Zhuo et al., 2017b); annual agricultural diffuse pollution contributed to more than 60,000 tonnes of the TP input in the Three Gorges Region between 1998 and 2011 (Zhang, 2015). Although turbid flood water discharge facilitated the transportation of nonpoint sources pollution during the wet season, efficient SS retention and abundant water column DP loads favored the enrichment of sediment P. Because of low flow velocity, discharging turbid flood water can only transport a part of the water column PP; this has a negligible contribution to transferring sediment accumulated P from the TGR to the downstream river reaches. Therefore, surface sediment in the TGR acts as a “sink” for P in the long term, even if turbid flood water is periodically discharged.

4. Conclusions

The TGR has a powerful SS retention capacity and tends to retain courser material. Release of turbid flood water has discharged approximately 20 % of the sediment inflow since impounding the TGR to 175 m. Sediment delivery ratio of the TGR is closely related to the operational water level in the flood season, and low operational water level and high upstream runoff favor SS discharge from the reservoir. Releasing turbid flood water has limited capacity for SS discharge and the deposited sediment volume has constantly increased in the TGR, at rate of 0.117 billion tonnes per year.

Muddy water discharge affects sediment physiochemical properties. Silt and fine sand dominated the surface sediment composition. MPS was larger for surface sediment obtained in the flood season than for surface sediment obtained during the dry season. The MPS tended to insignificantly increase with an increase in the column sediment depth of 0-20 cm. However, no obvious difference was observed in mineral components among the column sediment samples.

The TP content in surface sediment was 2.6 %–17.5 % lower in the turbid flood water releasing period than in the clean water storing period. Fast SS deposition rate and similar sediment physiochemical properties jointly resulted in a relatively uniform distribution of P fractions when sediment depth increased from 0 to 20 cm. Bio-P was weakly related to sediment MPS, but positively related to sediment OM, with a correlation coefficient of 0.50.

Because of the continuous increase in sediment deposition and decline in the inflow sediment particle size, the amount and content of P in surface sediment in the TGR might be increased when turbid flood water was discharged. Increasing water column DP input and a great amount of fine particle deposition resulted in the surface sediment in the TGR acting as a “sink” for P in the long term, even when turbid flood water was periodically released.

Acknowledgments

This study was supported by the The National Key Research and Development Program of China (Grant no. 2018YFC040760403), Central Public Interest Scientific Institution Basal Research Fund (Grant no. CKSF2017047/SH) and the National Natural Science Foundation of China (Grant no. 51379017 and 51409009). The authors greatly appreciate the anonymous reviewer’s excellent comments in improving the manuscript quality.

Reference

APHA ., 1998. Standard Methods for the Examination of Water and Wastewater, 20th ed. American Public Health Association/American Water Works Association/ Water Environment Federation, Washington DC, USA.

Cao, Z., Zhang, X., Ai, N., 2011. Effect of sediment on concentration of dissolved phosphorus in the Three Gorges Reservoir. International Journal of Sediment Research, 26, 87-95.

Chen, M., Ding, S., Liu, L., Xu, D., Gong, M., Tang, H., Zhang, C., 2016. Kinetics of phosphorus release from sediments and its relationship with iron speciation influenced by the mussel (Corbicula fluminea) bioturbation. Science of The Total Environment, 542, 833-840.

CWRC (Changjiang Water Resource Commission), 2000-2016. Changjiang Sediment Bulletin. Changjiang Press, Wuhan (in Chinese).

Fan, X., Ding, S., Gong, M., Chen, M., Gao, S., Jin, Z., Tsang, D. C. W., 2018. Different Influences of Bacterial Communities on Fe (III) Reduction and Phosphorus Availability in Sediments of the Cyanobacteria- and Macrophyte-Dominated Zones. Frontiers in Microbiology, 9 2636.

Fu, B. J., Wu, B.F., Lu, Y. H., Xu, Z. H., Cao, J. H., Niu, D., Yang, G. S., Zhou, Y. M., 2010. Three Gorges project: efforts and challenges for the environment. Progress in Physical Geography, 34, 741-754.

Han, C., Zheng, B., Qin, Y., Ma Y., Yang C., Liu Z., Cao W., Chi M., 2018. Impact of upstream river inputs and reservoir operation on phosphorus fractions in water-particulate phases in the Three Gorges Reservoir. Science of the Total Environment, 610-611,1546-1556.

Hu, J., Yang, S.F., Wang, X. Q., 2013. Sedimentation in Yangtze River above Three Gorges Project since 2003 Journal of Sediment Research, 1, 39-44 (in Chinese).

Huang, J. J., Wang, C., Fang, B., Feng, L., Fang, F., Li, Z., Guo, J. S., 2017. Characterization of phosphorus fractions in the soil of water-level-fluctuation zone and unflooded nankside in PengxiRiver, Three Gorges Reservoir. Environmental Science, 38, 3673-3681(in Chinese).

Huang, L., Fang, H., Reible, D., 2015. Mathematical model for interactions and transport of phosphorus and sediment in the Three Gorges Reservoir. Water Research. 85, 393-403.

Jarvie, H. P., Jurgens, M.D., Williams, R.J., Neal, C., Davies, J.J.L., Barrett, C., White, J., 2005. Role of river bed sediment as sources and sinks of phosphorus across two major eutrophic UK river basins: The Hampshire Avon and Herefordshire Wye. Journal of Hydrology, 304, 51–74.

Jin, X. C., Wang, S.R., Pang, Y., Wu, F. C., 2006. Phosphorus fractions and the effect of pH on the phosphorus release of the sediments from different trophic areas in Taihu Lake, China. Environmental Pollution, 139, 288–295.

Li, B., Cai, Q. H., Zhang, M., Shao, M. L., 2015a. Macroinvertebrate community succession in the Three-Gorges Reservoir ten years after impoundment.

Quaternary International, 380-381, 247-255.

Li, G. Y., Xiao, S. B., Wang, Y. C., Liu, L., Niu, F. X., 2012a. Distributional characteristics of grain size and mineral composition in sediments of Yangtze River in Three Gorges Reservoir. Journal of China Three Gorges University, 34, 9-13 (in Chinese).

Li, W. J., Yang S.F., Hu, J., Fu, X. H., 2015b. Preliminary analysis on the causes of silt deposition in the Three Gorges Reservoir. Journal of Sediment Research, 5, 7-13.

Liu, W., Wang, S., Zhang, L., Ni, Z., Zhao, H., Jiao, L., 2015. Phosphorus release characteristics of sediments in Erhai Lake and their impact on water quality. Environmental Earth Sciences, 74, 3753-3766.

Lou, B., Yin, S., Mu, H., Zhang, X., 2011. Comparison of total phosphorus concentration of Yangtze River within the Three Gorges Reservoir before and after impoundment. Journal of Lake Sciences, 23, 863-867 (in Chinese).

Luo, H. J., Liu, D.F., Huang, Y. P., 2015. Study on phosphorus characteristics in sediments of Xiangxi Bay, China Three-Gorge Reservoir. Water & Environment Journal, 6,281-289.

Mao, H.M., Liu, S.H., Zhou, H.Y., 2012. Preliminary analysis of sediment distribution in the Three Gorges Reservoir. Hydroscience and Engineering, 5, 67-71 (in Chinese).

Miller, M. P., 2012. The influence of reservoirs, climate, land use and hydrologic conditions on loads and chemical quality of dissolved organic carbon in the Colorado River. Water Reservoir Resource, 48, 810-830.

MWR (Ministry of Water Resource, P.R. China), 2006. Code for Reservoir Hydrologic and Sediment Survey (SL 339-2006), MWR. Beijing.

Pan, C.J., Li, R., Tang, X.Q., Xia, Z.Y., Li, Q.Y., Yang, W.J., Xu, W.N., 2018. Assessment of physicochemical properties and phosphorus fraction distribution characteristics in sediments after impoundment of the Three Gorges Reservoir to 175m, Environmental Science, 39, 111-119 (in Chinese).

Pan, T.T., Zhao, X., Yuan, Y. J., Song, H.Y., Zhu, K.X., Bi, Y.H., Hu, Z.Y., 2016 .Spatio-temporal distribution characteristics of different phosphorus forms in sediments from the Three Gorges Reservoir. Acta Scientiae Circumstantiae, 36, 2968-2973(in Chinese).

Ribeiro, D.C., Martins, G., Nogueira, R., Cruz, J.V., Brito, A.G., 2008. Phosphorus fractionation in volcanic lake sediments (Azores-Portugal). Chemosphere, 70, 1256-1263.

Ruban, V., López-Sánchez, J. F., Pardo, P., Rauret, G., Muntau, H., Quevauviller, P. H., 2001. Development of a harmonized phosphorus extraction procedure and certification of a sediment reference material. Journal of Environmental Monitoring, 3, 121-125.

Shen, J., Yuan, H., Liu, E., Wang, J., Wang, Y., 2011. Spatial distribution and stratigraphic characteristics of surface sediments in Taihu Lake, China. China. Science. Bulletin. 56, 179–187.

Tang X Q., Wu M., Li R.. 2018a. Distribution, sedimentation, and bioavailability of particulate phosphorus in the mainstream of the Three Gorges Reservoir. Water Research, 140, 44-55.

Tang X Q., Wu M., Li R.. 2018b. Phosphorus distribution and bioavailability dynamics in the mainstream water and surface sediment of the Three Gorges Reservoir between 2003 and 2010. Water Research, 10.1016/j.watres.2018.08.041.

Tang, X.Q., Wu, M., Dai, X.C., Chai, P.H., 2014. Phosphorus storage dynamics and adsorption characteristics for sediment from a drinking water source reservoir and its relation with sediment compositions. Ecological Engineering, 64, 276-284.

Wang, D., Ji, Z., Deng, A., He, F., Dong, Z., Wang, X., 2016. Regularity for sediment floc deposition in the Three Gorges Reservoir. Journal of Hydraulic Engineering, 47,1389-1397.

Wang, J.D., Sheng, Y.W., Gleason, C.J., Wada, Y., 2013. Downstream Yangtze River levels impacted by Three Gorges Dam. Environmental Research Letters, 8, 044012.

Wang, S.R., Jin, X.C., Zhao, H.C., Zhou, X.N., Wu, F.C., 2007. Effect of organic matter on the sorption of dissolved organic and inorganic phosphorus in lake sediments. Colloids and Surfaces A, 297, 154–162.

Wang, Y., Shen, Z.Y., Niu, J.F., Liu, R.M., 2009. Adsorption of phosphorus on sediments from the Three-Gorges Reservoir (China) and the relation with sediment compositions. Journal of Hazardous Materials, 162, 92-98.

Wang, Y.,Niu, F., Xiao, S., Liu, D., Chen, W., Wang, L., Yang, Z., Ji, D., Li, G., Guo, H., Li, Y., 2015. Phosphorus fractions and its summer's release flux from sediment in the China's Three Gorges Reservoir. Journal of Environmental Informatics, 25, 36-45.

Withers, P.J.A., Jarvie, H.P., 2008. Delivery and cycling of phosphorus in rivers: a review. Science of The Total Environment. 400, 379-395.

Wu, M., Huang, S.L., Wen, W., Sun, X.M., Tang, X.Q., Scholz, M., 2011. Nutrient distribution within and release from the contaminated sediment of Haihe River. Journal of Environmental Sciences, 23, 1086-1094.

Wu, Y., Wang, X., Zhou, J., Bing, H., Sun, H., Wang, J., 2016. The fate of phosphorus in sediments after the full operation of the Three Gorges Reservoir, China. Environmental Pollution, 214, 282-289.

Wu, Z., Liu, Y., Liang, Z., Wu, S., Guo, H., 2017. Internal cycling, not external loading, decides the nutrient limitation in eutrophic lake: a dynamic model with temporal Bayesian hierarchical inference. Water Research. 116, 231–240.

Xiao, X.C., 2015. Agricultural non-point source pollution control in the Three Gorges Region. Southwest University, Chongqing (in Chinese).

Xing, X., Ding, S., Liu, L., Chen, M., Yan, W., Zhao, L., Zhang, C., 2018. Direct evidence for the enhanced acquisition of phosphorus in the rhizosphere of aquatic plants: A case study on Vallisneria natans. Science of The Total Environment, 616-617, 386-396.

Yao, Q.Z., Du, J.T., Chen, H.T., Yu, Z.G., 2016. Particle-size distribution and phosphorus forms as a function of hydrological forcing in the Yellow River. Environmental Science and Pollution Research, 23, 3385-3398.

Yao, S.C., Xue, B., Li, S.J., Liu, J.F., Xia, W.L., 2006. Sedimentation rates in Honghu, Chaohu and Taihu lakes in the middle and lower reaches of the Yangtze River. Resources and Environment in the Yangtze Basin, 15, 569-573 (in Chinese).

Zhang, L., Wang, J.Q., Ma, Y.P., Chen, R., Ren, A.H., 2012a. Phosphorus forms of different weathering degree rocks in Chaohu Lake area. China Environmental Science, 32, 1820-1825(in Chinese).

Zhang, M., Xu, Y., Shao, M., Cai, Q., 2012b. Sedimentary nutrients in the mainstream and its five tributary bays of a large subtropical reservoir (Three Gorges Reservoir, China). Quaternary International, 282, 171-177

Zhou, Q., Gibson, C.E., Zhu, Y., 2001. Evaluation of phosphorus bioavailability in sediments of three contrasting lakes in China and the UK. Chemosphere, 42,221-225.

Zhuo, H.H., Qiu, G.S., Zhai, W.Y., Liu Y.B., Lan, J., 2017a. Evaluation of temporal and spatial variation characteristics of nutrients in surface sediment of Three Gorges Reservoir area. Environmental Science, 38, 5020-5031(in Chinese).

Zhuo, H.H., Sun, Z.W., Zheng, H.Y., Liu, M.X., Wu, Y.L., Lan, J., 2017b. Analysis on source and variation trends of pollutants in Three Gorges Reservoir. Yangtze River , 48,13-18 (in Chinese).

Figure captions

Fig. 1 Location of sampling sites along the mainstream sections of the TGR

Fig. 2 Sediment delivery ratio, accumulated deposition volume, and annual sediment flux between 2004 and 2016

Fig. 3 Variation in surface sediment MPS and OM column in October 2016, June 2017, and December 2017

Fig. 4 Vertical distribution of OM, MPS, and major components for representative column sediment samples of YY

Fig. 5 Variation in surface sediment TP, Fe/Al-P, and TP in October 2016, June 2017, and December 2017

Fig. 6 Vertical distribution of different P fractions for representative column sediment samples from YY

Fig. 7 Relationship between Bio-P and OM and MPS for column sediment samples

Fig. 8 Typical deposition cross-section profile for the TGR a the distance of (a) 5.6 km, (b) 160.1 km, and (c) 431.3 km to the TGD in October 2003, 2011, and 2012, respectively

Table 1. Flow, water level and sediment delivery ratio in the TGR between June and September

Year	Average water level (m)	Flood peak flow (m^3/s)	Daily average flow (m^3/s)	Sediment delivery ratio (%)
2003	135.10	47590	24999	40.74
2004	135.60	62860	21414	39.07
2005	135.50	48600	24925	42.22
2006	135.70	29840	12937	9.49
2007	144.70	45410	22978	25.26
2008	145.60	36820	21786	16.90
2009	147.20	53920	21517	21.71
2010	153.60	64360	24294	15.99

Table 2. Variation of sediment transportation characteristics between the pre- and post-TGR period

Controlled sections	Annual average SS flux (billion tonne)		Annual average SS concentrations (kg/m^3)		Annual average SS MPS (μm)	
	Pre-TGR	Post-TGR	Pre-TGR	Post-TGR	Pre-TGR	Post-TGR
Cuntan	0.43 (1953-2002)	0.20 (2003-2010)	1.24 (1953-2002)	0.60 (2003-2010)	0.011 (1987-2002)	0.009 (2003-2010)
Yichang	0.49 (1950-2002)	0.05 (2003-2010)	1.13 (1950-2002)	0.14 (2003-2010)	0.009 (1987-2002)	0.004 (2003-2010)

SS, suspended sediment; MPS, median particle size; duration provided in parenthesis.

Table 3. Means and standard deviations for major physiochemical properties of column sediment in the mainstream sections of the Changjiang River (n = 10)

Sampling sites	MPS (μm)	OM (%)	pH	Proportions of mineral component (%)			
				chlorite	illite	quartz	Others*
YY (Yunyang)	7.78±2.71	2.44±0.79	7.59±0.08	26.80±2.62	23.90±3.00	24.00±1.76	25.30±4.50
FJ (Fengjie)	5.81±1.13	3.56±0.54	7.39±0.07	29.10±2.08	25.60±2.59	22.10±1.10	23.20±3.58
BD (Badong)	6.38±2.18	3.31±0.62	7.56±0.07	27.30±3.56	22.10±4.07	23.30±1.77	27.30±6.13
XX (Xiangxi)	7.50±2.49	3.50±0.42	7.50±0.06	26.00±3.27	19.90±3.96	23.60±0.84	30.50±5.93
ZG (Zigui)	5.38±0.47	4.35±0.61	7.44±0.06	31.00±2.16	28.00±2.31	21.30±0.67	19.70±3.71

* Other mineral components, including feldspar, calcite, dolomite, amphibole, and iron pyrite.

MPS, median particle size; OM, organic matter.

Table 4. Means and standard deviations for fractional phosphorus contents of column sediment in the mainstream sections of the Changjiang River (n = 10)

Sampling sites	Phosphorus content (mg/kg)						
	Ex-P	Al-P	Fe-P	O-P	Ca-P	TP	Bio-P
YY (Yunyang)	9.35±1.89	27.31± 5.22	1.33±0.25	301.59 ±53.84	601.90±73.73	983.76±20.65	38.00 ±6.65
FJ (Fengjie)	8.47±1.10	33.64±6.83	1.03±0.98	287.66±41.20	505.30±39.57	939.26±28.70	43.13±6.20
BD (Badong)	9.05±1.60	30.54±5.14	1.13±0.46	329.39±14.36	542.04±41.23	893.05±19.24	40.72±6.22
XX (Xiangxi)	9.88±2.59	39.96±4.13	1.43±0.52	305.94±15.62	551.20±67.70	965.74±32.98	51.27±4.99
ZG (Zigui)	8.77±0.71	45.66±3.69	0.63±0.32	340.02±39.85	481.03±72.22	901.51±21.71	55.06±3.90

P, phosphorous; Ex-P, exchangeable P; Al-P, Al oxide-bound P; Fe-P, Fe oxide-bound P; O-P, occluded P; TP, total P; Bio-P, bioavailable P.

Highlights

- Sediment deposition constantly increased at a rate of 0.117 billion tonnes per year.
- Sediment particle sizes were larger in the flood season than in the dry season.
- No obvious phosphorus enrichment occurred in the top 20 cm of column sediment.
- Sediment in the Three Gorges Reservoir acts as a “sink” for phosphorus

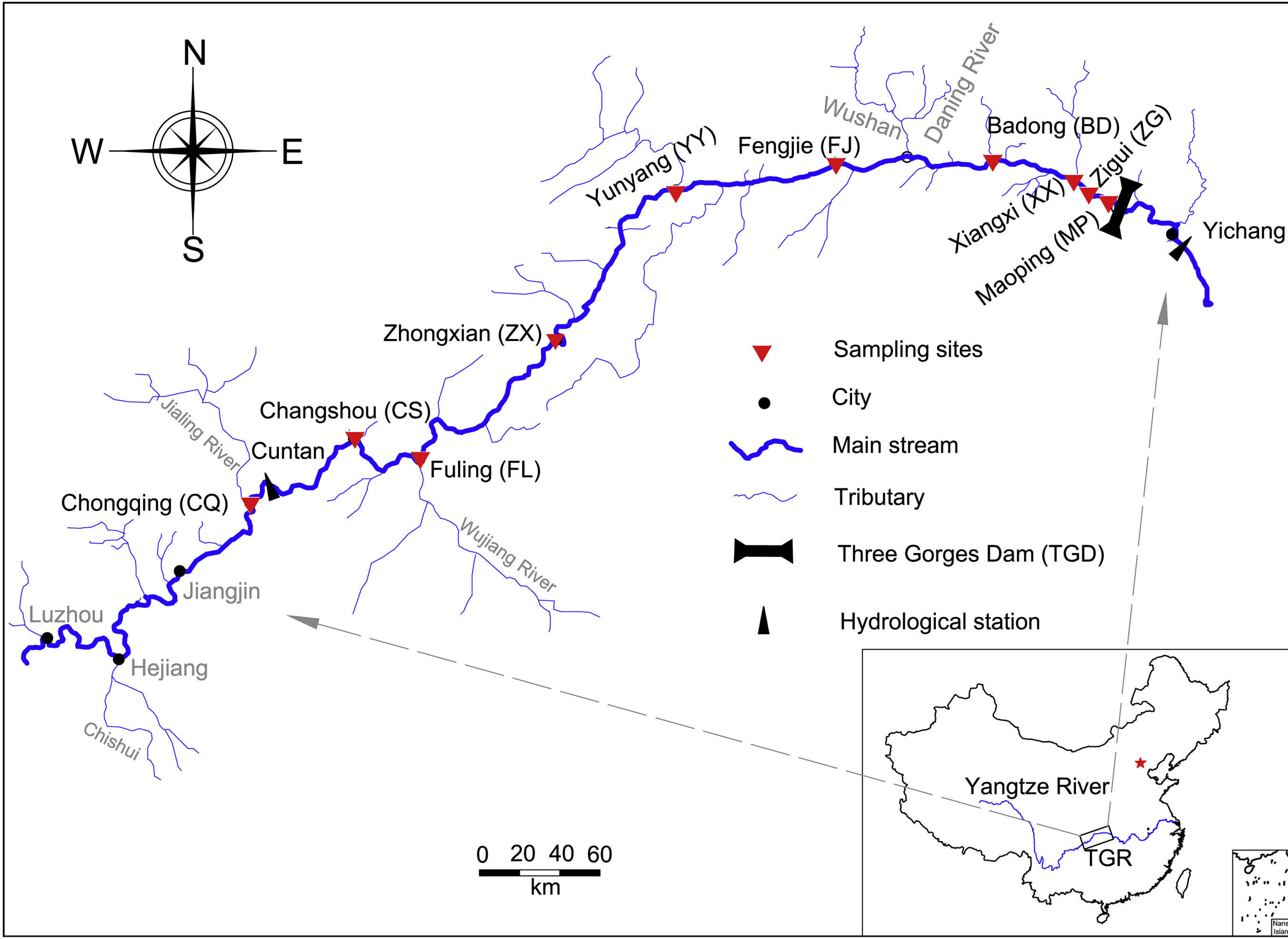
N
S
W
E
Yunyang (YY)
Fengjie (FJ)
Wushan
Daning River
Badong (BD)
Zigui (ZG)
Xiangxi (XX)
Maoping (MP)
Yichang
Zhongxian (ZX)
Changshou (CS)
Cuntan
Fuling (FL)
Chongqing (CQ)
Jialing River
Wujiang River
Jiangjin
Luzhou
Hejiang
Chishui
Sampling sites
City
Main stream
Tributary
Three Gorges Dam (TGD)
Hydrological station
0 20 40 60
km
Yangtze River
TGR
Nansha Islands

Figure 1

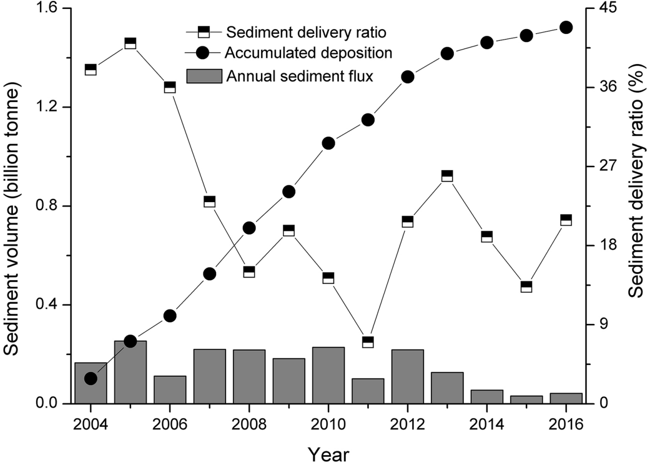
1.6
1.2
0.8
0.4
0.0
Sediment volume (billion tonne)
45
36
27
18
9
0
Sediment delivery ratio (%)
Sediment delivery ratio
Accumulated deposition
Annual sediment flux
2004
2006
2008
2010
2012
2014
2016
Year

Figure 2

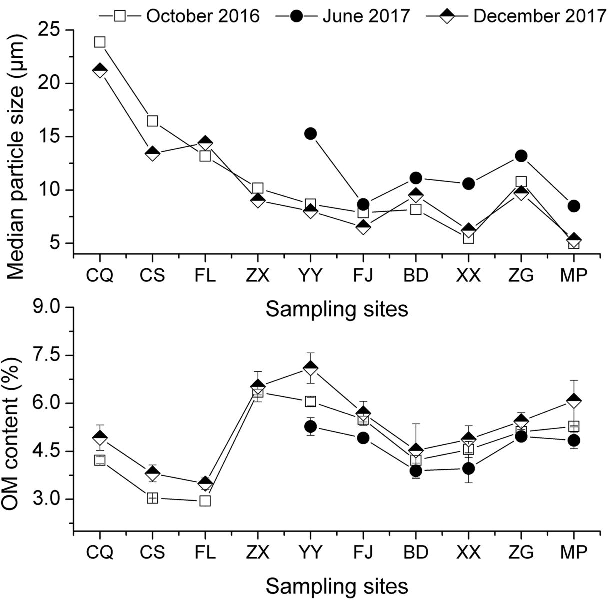
October 2016
June 2017
December 2017
Median particle size (μm)
25
20
15
10
5
CQ
CS
FL
ZX
YY
FJ
BD
XX
ZG
MP
Sampling sites
OM content (%)
9.0
7.5
6.0
4.5
3.0
CQ
CS
FL
ZX
YY
FJ
BD
XX
ZG
MP
Sampling sites

Figure 3

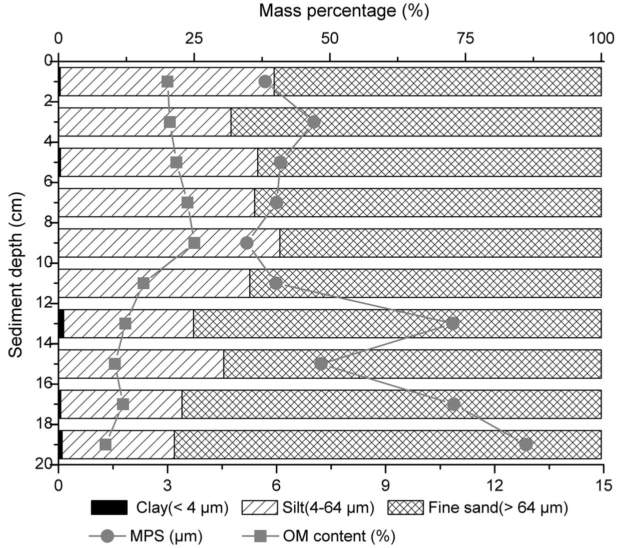

Mass percentage (%)
0
25
50
75
100
Sediment depth (cm)
0
2
4
6
8
10
12
14
16
18
20
0
3
6
9
12
15
Clay(< 4 μm)
Silt(4-64 μm)
Fine sand(> 64 μm)
MPS (μm)
OM content (%)

Figure 4

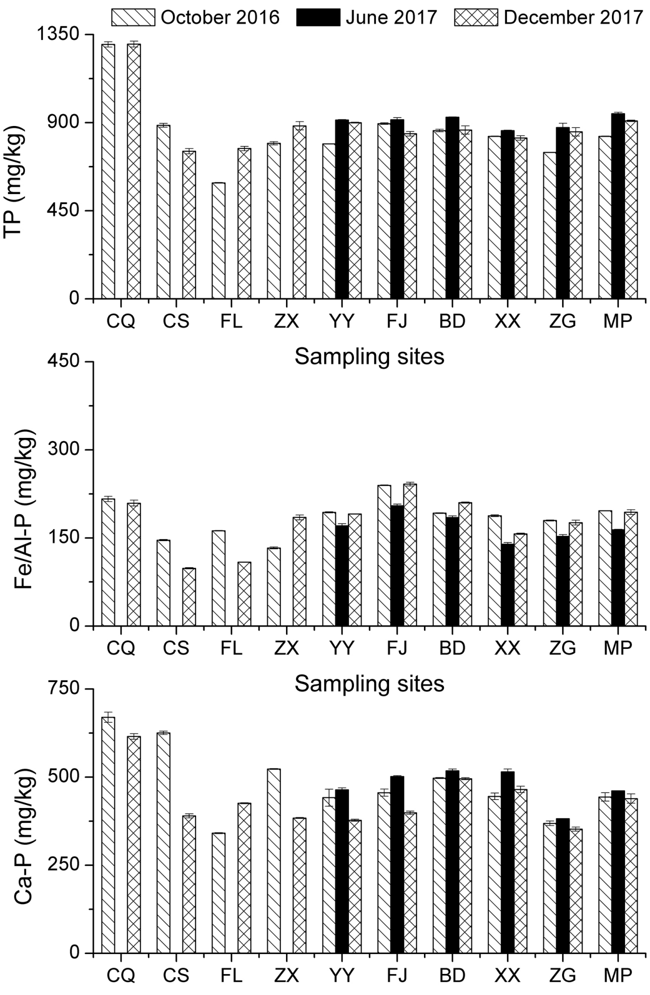
October 2016
June 2017
December 2017
TP (mg/kg)
1350
900
450
0
CQ
CS
FL
ZX
YY
FJ
BD
XX
ZG
MP
Sampling sites
Fe/Al-P (mg/kg)
450
300
150
0
CQ
CS
FL
ZX
YY
FJ
BD
XX
ZG
MP
Sampling sites
Ca-P (mg/kg)
750
500
250
0
CQ
CS
FL
ZX
YY
FJ
BD
XX
ZG
MP
Sampling sites

Figure 5

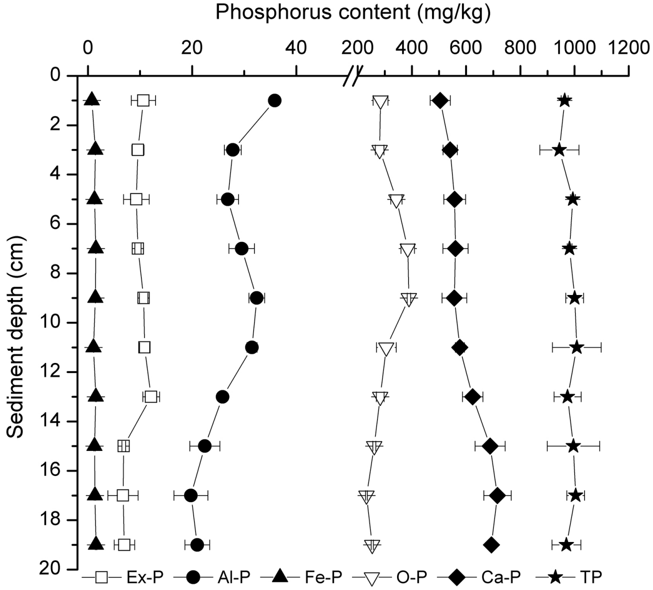
Phosphorus content (mg/kg)
0
20
40
200
400
600
800
1000
1200
Sediment depth (cm)
0
2
4
6
8
10
12
14
16
18
20
Ex-P
Al-P
Fe-P
O-P
Ca-P
TP

Figure 6

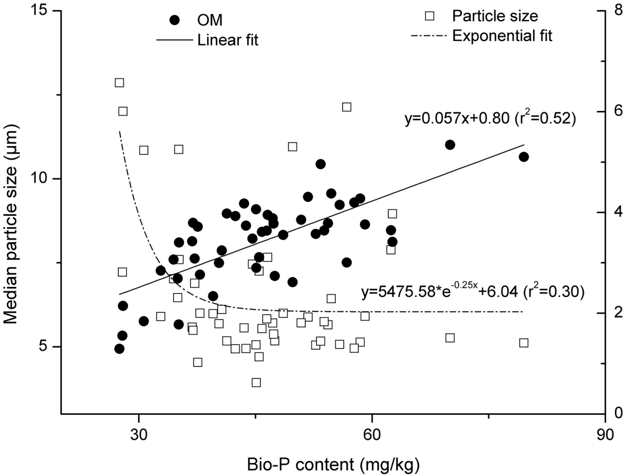

OM
Linear fit
Particle size
Exponential fit
y=0.057x+0.80 (r2=0.52)
y=5475.58*e-0.25x+6.04 (r2=0.30)
Median particle size (μm)
Sediment OM content (%)
Bio-P content (mg/kg)
15
10
5
8
6
4
2
0
30
60
90

Figure 7

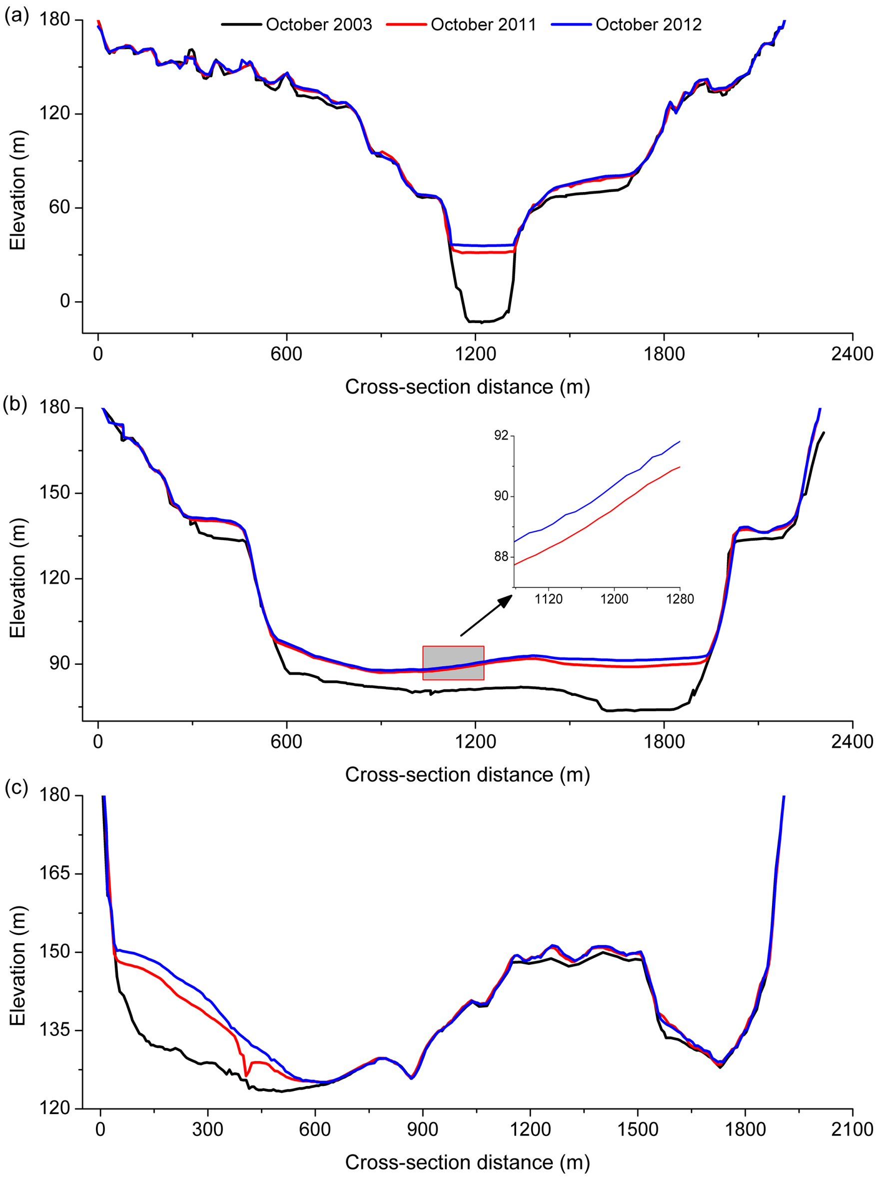
(a)
October 2003
October 2011
October 2012
180
120
60
0
Elevation (m)
0
600
1200
1800
2400
Cross-section distance (m)
(b)
180
150
120
90
Elevation (m)
92
90
88
1120
1200
1280
0
600
1200
1800
2400
Cross-section distance (m)
(c)
180
165
150
135
120
Elevation (m)
0
300
600
900
1200
1500
1800
2100
Cross-section distance (m)

Figure 8